Classification of the nonlinear dynamics in an initially curved bistable micro/nano-electro-mechanical system resonator

Farid Tajaddodianfar[1], *Mohammad Reza Hairi Yazdi*[1], *Hossein Nejat Pishkenari*[2], *Ehsan Maani Miandoab*[1], *Hassen M. Ouakad*[3]

[1]*School of Mechanical Engineering, College of Engineering, University of Tehran, Tehran, Iran*
[2]*School of Mechanical Engineering, Sharif University of Technology, Tehran, Iran*
[3]*Department of Mechanical Engineering, King Fahd University of Petroleum and Minerals, Dhahran, Kingdom of Saudi Arabia*
E-mail: myazdi@ut.ac.ir

Published in Micro & Nano Letters; Received on 12th March 2015; Accepted on 15th July 2015

The nonlinear dynamics of a bistable micro/nano-electro-mechanical system resonator composed of an arch-shaped microbeam is investigated. The initially curved microbeam is actuated through a combined DC and AC electrostatic parallel plate field. A single degree of freedom model obtained using the Galerkin's decomposition method with distributed electrostatic force is implemented in order to investigate the resonator dynamics near its primary resonance. According to the shape of the potential energy function which depends on the system parameters, the nonlinear dynamics of the system are classified into certain categories. The appearance of various nonlinear phenomena including dynamic snap-through, dynamic pull-in, chaotic or large amplitude vibrations, hysteresis and softening-type behaviours are discussed within the introduced categories. A typical case scrutinised on detail, showing consequent snap-through instabilities which are responsible for transitions between the present stable configurations of the arch-shaped microbeam. Details of the resulting hysteresis loop governing these transitions are discussed. Moreover, discussion is provided about the formation of the hysteresis loops which can affect the filtering functionality of the proposed bistable MEMS resonator.

1. Introduction: Bistable MEMS devices have attracted a growing attention in the research community in recent years. Numerous investigations were motivated by the interesting applications of bistable MEMS devices such as microrelays [1], actuators [2], switches [3], MEMS-based mechanical memory [4] etc. The system capability to operate in more than one stable configuration at fixed values of the parameters is referred to as bistability. A MEMS device comprised of an initially curved shallow microbeam can be categorised as in the so-called family of bistable devices. These mechanically bistable MEMS devices are vulnerable to a nonlinear phenomenon, namely, snap-through, which is responsible for the mechanical transitions of the micro arch between its stable configurations.

Some researchers have investigated the static snap-through response in electrostatically actuated bistable MEMS devices. Zhang *et al.* [5] studied experimentally the bistability of an initially curved micro-machined beam. They introduced snap-through as a no-power-consuming mechanical jump without pull-in which can be implemented in the development of highly sensitive sensors. Krylov *et al.* [6–9] have reported analytical and experimental investigations on the dynamics of initially curved MEMS. Finite element and boundary element methods were implemented in the work of Das and Batra [10], as part of treat as an attempt to study pull-in and snap-through instabilities. Mohammad and Ouakad [11] have recently discussed the dynamics of a free-of-pull-in arch MEMS actuated by fringing electrostatic fields.

A few groups have focused on the resonant behaviours of bistable arch-shaped microbeams. Casals-Terre *et al.* [12] presented an arch-shaped double clamped microbeam under combined DC and AC electrostatic actuations. Ouakad and Younis [13] studied an arch-shaped MEMS resonator. They studied the dynamic behaviour of the resonator by the Galerkin projection method. Moreover, they implemented the multiple scales method to study the response of the resonator under small DC and AC actuations. Younis *et al.* [14] investigated theoretically and experimentally an arch-shaped MEMS resonator. They studied various nonlinear phenomena including dynamic snap-through and pull-in, via their simulations and the reported experimental data. They also suggested these types of MEMS to be used as low-powered switches or bandpass filters. In recent investigations, Ouakad [15] and Ouakad and Younis [16] have reported further discussion on the application of these types of MEMS as bandpass filters. Furthermore, the present authors have proposed an analytical approach, namely, the homotopy analysis method, for the study of the nonlinear frequency response of arch MEMS resonators [17]. Moreover, in a recent work [18], we have focused only on the possibility of chaotic vibrations in arch MEMS resonators, and we have discussed the effects of various parameters on the formation of chaotic behaviours.

The above state-of-the-art summary of the dynamics of arch-shaped MEMS resonators reveals a need for a further and deep study of the nonlinear dynamics of these micro-systems. In other words, comprehensive work seems to be needed in order to verify the conditions in which various nonlinear phenomena can possibly take place. These phenomena include dynamic snap-through, dynamic pull-in, hysteresis, softening behaviour and large amplitude limit cycles or chaotic vibrations. Note that the present Letter is clearly different from the authors' previous works since only bistable [17] and chaotic [18] vibrations are proposed in our previous works, while the possibility of the appearance of all other nonlinear phenomena is discussed in this Letter.

In this Letter, we present a classification for the non-linear dynamics of an arch-shaped resonator. For this, we classify the dynamic behaviours according to the shape of the resonator's potential energy function. It is assumed that a double clamped micro arch under combined DC and AC electrostatic actuations acts as a resonator near its first fundamental frequency. The shape of the potential energy function, which helps to classify the nonlinear dynamics of the micro arch depends on its geometrical parameters and the applied DC voltage. Other parameters such as the damping and the AC load are determinant in the formation of the

behaviour of the micro-system. The possibility of the appearance of nonlinear phenomena is studied in each classification category. We show that, for each of the nonlinear behaviours, certain conditions need to be satisfied. For instance, requirements for the filtering functionality of the investigated bistable MEMS are satisfied only in one of the investigated categories. Moreover, we propose the formation of hysteresis loops in the frequency response of the system, and show that such a nonlinear behaviour can critically affect the recently proposed filtering functionality of the system. This Letter continues with the presentation of the mathematical model in Section 2. Classifications of the nonlinear dynamics of the investigated curved microbeam are given in Section 3. This Letter ends with our conclusions in Section 4.

2. Mathematical modelling: An initially curved microbeam, as schematically shown in Fig. 1, is considered in this Letter. An electrostatic load imposes a lateral deflection of the arch which is governed by a partial differential equation on the basis of the Euler-Bernoulli and shallow arch assumptions. Implementing the first-mode Galerkin projection method, one is left with a nonlinear ordinary differential equation governing the first modal displacement of the arch q as a function of non-dimensional time τ

$$\frac{\mathrm{d}^2q}{\mathrm{d}\tau^2}+\mu\frac{\mathrm{d}q}{\mathrm{d}\tau}+F(q)=0,$$
$$F(q)=(1+2h^2\bar{\alpha})q-3\bar{\alpha}hq^2+\bar{\alpha}q^3-\frac{\beta(1+2R\cos(\omega_0\tau))}{2\alpha_{10}\sqrt{(1+h-q)^3}} \quad (1)$$

where $\bar{\alpha}$ is the non-dimensional stretching parameter, α_{10} is a constant and μ represents damping effects. Moreover, h, β, R and ω_0 stand for the non-dimensional initial elevation, DC voltage, DC–AC voltage ratio and actuation frequency, respectively. For definition of the so-called parameters as a function of the resonator's geometry and material, and for details of its derivation, see [17, 18].

For the study of the resonance behaviour of the arch near its first fundamental frequency, we assume that ω_0 is given by

$$\omega_0=\lambda+\sigma,\ \lambda^2=\left.\frac{\partial F}{\partial q}\right|_{\substack{q=q_{01}\\R=0}} \quad (2)$$

It will be shown later in this investigation that the potential function plays an important role in the initiation of various nonlinear dynamic behaviours of the micro-arch resonator. Before further discussing this, we start by calculating the potential function of the micro-resonator in this Section. To derive this function, we first eliminate the damping term from (6) as well as the AC loading term. Then, the potential function $U(q)$ can easily be calculated by integrating $F(q)$ neglecting the effect of R

$$U(q)=\left(\frac{1}{2}+\bar{\alpha}h^2\right)q^2-\bar{\alpha}hq^3+\frac{\bar{\alpha}}{4}q^4-\frac{\beta}{\alpha_{10}\sqrt{1+h-q}} \quad (3)$$

It is clear that the shape of potential function depends on β and h.

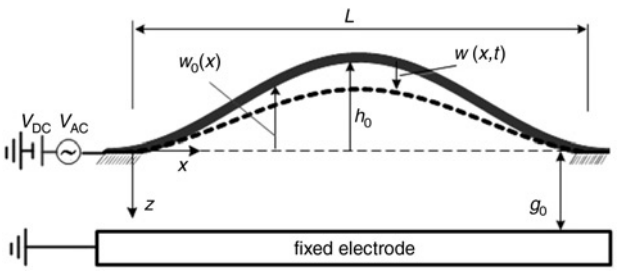

Figure 1 *Schematic of the arch resonator*

Label	Number of fixed points	Total description	Potential Function	Phase Plane
Category A	2	$U(q_{01})<U(q_p)$		
Category B	4	$U(q_{01})\simeq U(q_{02})<U(q_v)<U(q_p)$		
Category C	4	$U(q_{01})<U(q_{02})<U(q_v)<U(q_p)$ Or $U(q_{02})<U(q_{01})<U(q_v)<U(q_p)$		
Category D	4	$U(q_p)<U(q_v)$		

Figure 2 *Classification of the shapes of potential function*

Moreover, extremums of $U(q)$ are equal to the fixed points of (1). Thus, for various values of β and h, various numbers of minima and maxima appear in the potential function. For certain values of $h>h^*$ for which bistability occurs [9], different shapes of $U(q)$ are possible depending on the applied DC voltage parameter. We classify the possible potential function shapes into four major categories in Fig. 2. Note that both q_{01} and q_{02} address the stable fixed points, where q_s and q_p represent unstable fixed points relating to the snap-through and the pull-in instabilities, respectively.

3. Classification of dynamic behaviour: For certain values of the arch initial rise h and an applied DC voltage β, the shape of the potential function is qualitatively similar to one of the four cases of Fig. 2. However, the exact dynamic behaviour of the system depends on the other parameters including the AC voltage load described by parameter R, its forcing frequency detuning parameter σ and the damping coefficient μ.

In the next subsections, we discuss the various dynamic behaviours of the system for each of the four categories of Fig. 2. For each case, we examine various dynamic forcing conditions of the applied AC load and damping. Then we study a micro arch-shaped beam of length $L=1000$ μm, thickness $d=3$ μm, width $b=30$ μm and gap $g_0=10$ μm, which contribute to the constants of $\bar{\alpha}=7.993$ and $\alpha_{10}=198.436$.

3.1. Category A: As shown in Fig. 2, category A represents the condition for which either h is lower than h^*, forming only one stable fixed point or β is lower than the bistability condition. In other words, in the phase plane of the system a centre representing the stable fixed point and a saddle representing the unstable fixed point exist. In this case, for sufficiently low values of R and high values of μ, vibrations in the phase plane are enclosed by the homoclinic orbit corresponding to the pull-in saddle node. Hence, the maximum allowable response amplitude $a_{\max}$ is equal to the amplitude of the homoclinic orbit. Fig. 3 shows the frequency response in this case for $h=0.38$, $\beta=90$, $R=0.02$ and $\mu=0.02$. Note that for obtaining these frequency responses, only values of σ changing from a negative value to a positive value and vice versa are considered. Hence, the steady-state amplitude as well as the arch mean vibration value is recorded at each step.

3.2. Category B: The phase plane corresponding to category B consists of two centres representing the stable fixed points as well as two saddle nodes representing snap-through and pull-in instabilities as in Fig. 2. In this particular case, which is typically represented by $h=0.34$ and $\beta=130$, the potential function possesses a larger potential at the pull-in saddle node than that of the snap-through saddle node. Thus, the snap-through instability occurs first without any pull-in instability. Hence, snap-through instability is possible to occur over and over, making it a possible configuration undergoing a chaotic vibration. Depending on the

doi: 10.1049/mnl.2015.0087

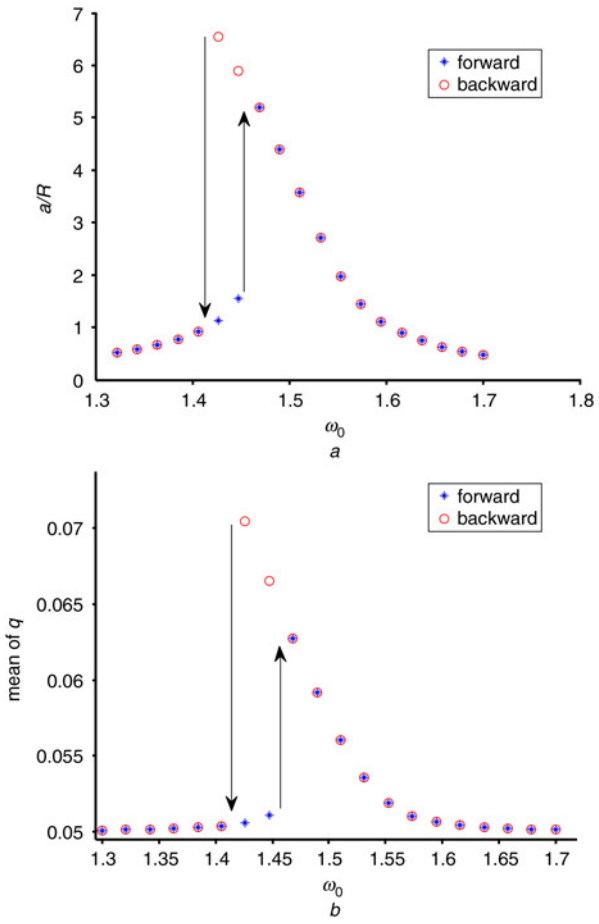

Figure 3 *Typical frequency response for Case A*
a Ratio of the output amplitude to input amplitude parameter R against frequency of the applied AC load
b Corresponding mean of the vibration against frequency

forcing amplitude as well as the damping coefficient, four types of dynamic behaviours are possible in this particular category, which can be summarised as follows.

Case B.1: For small values of R (AC load) or high values of μ (damping), the amplitude of the arch dynamic response does not exceed the critical amplitude of the snap-through homoclinic orbit. This behaviour is qualitatively similar to that discussed in category A and shown in Fig. 3, with some differences in the jump frequencies.
Case B.2: For relatively high values of R (AC load), the arch dynamic response amplitude exceeds the critical snap-through homoclinic amplitude, making it possible for the snap-through to occur. Since the potential of the two centres are almost same, it is possible for the system to snap back to the domain of attraction of the initial centre. This may lead to a possible steady-state chaotic behaviour as discussed in detail previously [18].
Case B.3: It is possible for the dynamic response amplitude to exceed the critical snap-through value while being lower than the pull-in critical value. This allows a larger amplitude of vibrations to appear by passing the two fixed points periodically as shown in Fig. 4 which is obtained for values of $R = 0.032$, $\mu = 0.013$ and $\sigma = -0.21$.

Under forward and backward frequency sweeps, hardening behaviour of the system under large amplitude vibrations is depicted in Fig. 5, where for the system parameters of Case B.3, simulations are performed to obtain the steady-state frequency response. For this, only the forcing frequency is tuned in backward and forward directions. Then, for each frequency, the mean as well as the

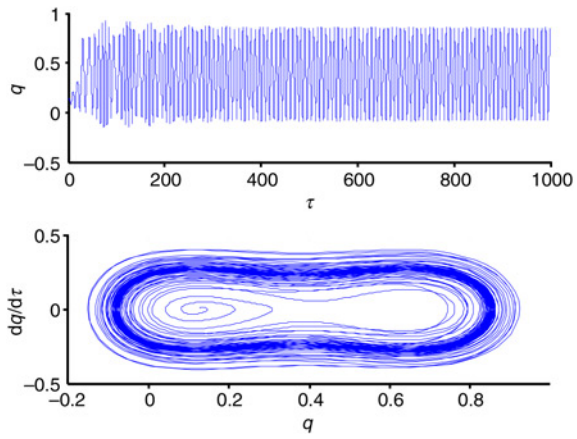

Figure 4 *Time series response and corresponding phase plane for the large amplitude vibrations for the Case B.3*

amplitude of dynamic vibrations are recorded. It is clear that the system shows a hardening type of behaviour for large amplitude vibrations corresponding to a larger mean of vibration. This can be a justification for what has been reported in previous works [13, 14].

Case B.4: With further increasing the amplitude of the AC actuation or decreasing the value of damping parameter, big values of the dynamic response amplitude are recorded. This causes the system

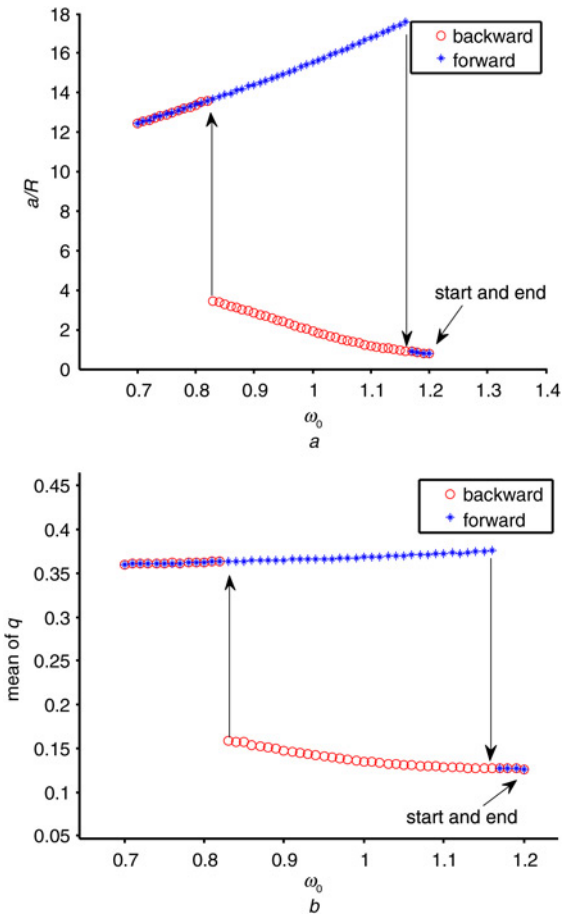

Figure 5 *System response under backward and forward frequency sweeps for Case B.3*
a Amplitude ratio
b Mean of vibrations

to reach the critical amplitude imposed by the pull-in homoclinic orbit, and consequently leads to pull-in.

3.3. Category C: As shown in Fig. 2, category C represents the condition for which two centres and two saddle nodes exist in the phase plane. The key feature of this particular case, which is represented by typical values of $h = 0.38$ and $\beta = 117$, is that the potential of the pull-in saddle node is larger than that of snap-through saddle node. Moreover, the potential of one of the stable centres is lower than the other. This leads to a possible snap-through motion without any pull-in and with possible transition between the stable points. Now, depending on the forcing amplitude as well as the damping coefficient, three types of dynamic behaviour are possible in this particular category, which can be summarised as follows.

Case C.1: For relatively small values of R (AC load) or for high values of μ (damping), the dynamic response amplitudes for this category do not exceed the snap-through critical value. As a consequence, a classical softening behaviour is expected in this particular case.

Case C.2: When R is selected sufficiently large to cause the resonance response amplitude to reach the critical snap-through amplitude, it is possible for the resonator to jump to the domain of attraction of the next centre due to the snap-through motion. Moreover, it is possible for the system to jump between the two stable domains of attraction. To study these stable transitions in detail, we have proposed four types of simulations for this particular case [17]:

1. Around the lower fixed point starting with large frequencies.
2. Around the higher fixed point starting with large frequencies.
3. Around the lower fixed point starting with small frequencies.
4. Around the higher fixed point starting with small frequencies.

In all of the above considered different simulations, the applied forcing frequency is selected close to the fundamental natural frequency of the arch. Fig. 6 displays the mean of the dynamic vibrations against applied forward and backward frequency sweeps for the above four simulation cases. Values of $h = 0.38$, $\beta = 157$, $R =$ 0.022 and $\mu = 0.03$ are used in these cases. Fig. 6 shows interesting dynamic behaviour of the transitions between the two stable solutions. These transitions are due to the dynamic snap-through occurring due to the resonance around each stable configuration. The other interesting behaviour is the sharp roll-off frequencies shown in Fig. 6. Tajaddodianfar *et al.* [17] have proposed the so-called sharp roll-off frequencies in four types, as given in Table 1; values of which are associated with simulations of Fig. 6.

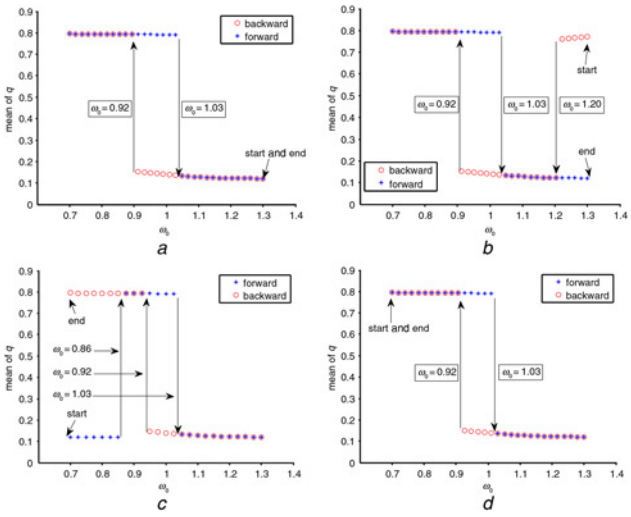

Figure 6 *Mean of the vibrations against applied frequency in forward and backward frequency sweeps of Case C.2*
a Type 1 simulations
b Type 2 simulations
c Type 3 simulations
d Type 4 simulations

Table 1 Critical frequencies and their definitions for Case C.2

Critical frequency	Explanation
$\omega_{LHL} = 0.86$	jump from the lower to higher fixed point in the forward frequency sweep path
$\omega_{LHR} = 0.92$	jump from lower to higher fixed point in the backward frequency sweep path
$\omega_{HLL} = 1.03$	jump from higher to lower fixed point the forward frequency sweep path
$\omega_{HLR} = 1.20$	jump from higher to lower fixed point in the backward frequency sweep path

For detailed description of each simulation see [17].

Analysis of the given four types of simulations reveals the following points for these types of behaviours:

1. It seems that there exist two softening type frequency responses, each one corresponding to one of the stable fixed points. The total frequency response is obtained by combination of the two frequency responses. Transition between the branches of the two responses occurs in the neighbourhood of the critical frequencies. Note that the necessary condition for these transitions is that the response amplitude given by each of the frequency response reaches the critical amplitude of the homoclinic orbit. For an analytical approach for the derivation of these frequency responses, see [17].
2. The whole frequency responses shown in Figs. 6*a* and *d* are the same, and constitute a closed hysteresis loop which can be passed repeatedly only by varying the actuating frequency. However, the frequency responses shown in Figs. 6*b* and *c* do not form a closed cycle. The other result is that, in case of repeating the actuating cycle in Figs. 6*b* or *c*, they are transformed to what is shown in Figs. 6*a* or *d*. Thus, we can infer that the response shown in Fig. 6*a* is dominant.
3. For development of the interesting behaviour in Case C.2, the potential function value of one of the fixed points should not be too small with respect to the other one. Otherwise, the critical amplitude of the snap-through homoclinic orbit grows and hence would be unreachable by the fixed AC load value. This definitely can prevent repeatable transitions between the stable fixed points.
4. When the response of the resonator obtained either at the backward frequency sweep in Fig. 6*b* or at the forward frequency sweep in Fig. 6*c* is considered, the functionality of the resonator as a bandpass filter is concluded. However, the four types of simulations performed in this Section suggest that the total behaviour of the system is different, forming a hysteresis loop which can affect the filtering functionality. This is a critical point which should be considered in the application of bistable MEMS as bandpass filters [15, 16].
5. Simulations show that the system response in forward and backward frequency sweeps is can possibly to be different. This has been observed experimentally by Oukad and Younis [16]. Thus, the proposed simulations can be interpreted as the justifications for what is already observed experimentally.

Case C.3: For certain values of parameters R, σ and μ, it is possible to form a condition for which the dynamic response amplitude would be larger than the critical values of the snap-through homoclinic orbits, but less than that of the pull-in instability. In this case,

doi: 10.1049/mnl.2015.0087

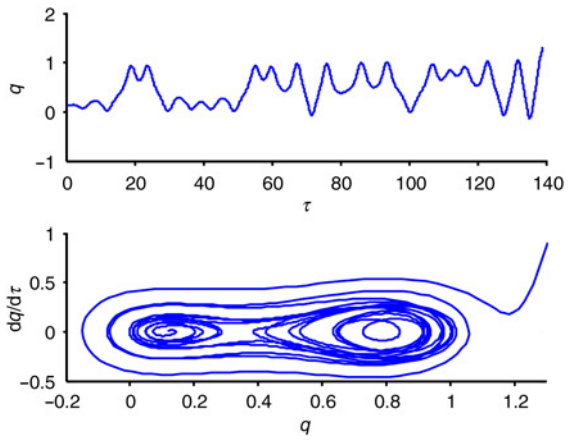

Figure 7 *Time series response and corresponding phase plane for Case C.4 undergoing dynamic pull-in*

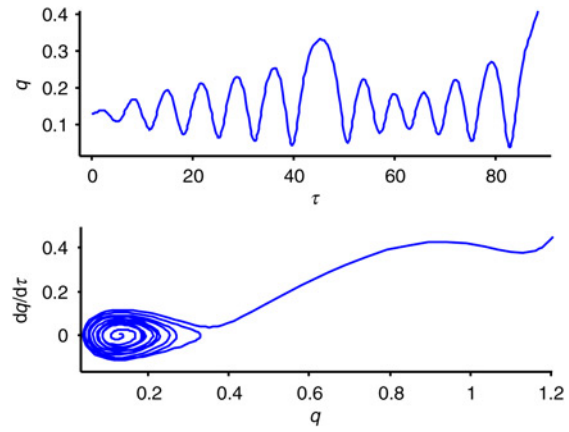

Figure 8 *Time series response and corresponding phase plane for Case D.2 undergoing dynamic pull-in*

a large periodic amplitude behaviour is expected. This is qualitatively similar to what is depicted in Fig 4 and discussed. The large amplitude vibrations were basically obtained for the following values: $R = 0.03$ $\mu = 0.015$ and $\sigma = -0.19$.

Case C.4: With further increase in R or decrease in μ with respect to Case C.3, dynamic vibrations reach the critical amplitude of the pull-in homoclinic orbit. This case is mainly describing the pull-in instability scenario that we got using the following values: $R = 0.04$, $\mu = 0.01$ and $\sigma = -0.19$. This is shown in Fig. 7.

3.4. Category D: As shown in Fig. 2, the main characteristic of this category is that the potential of the pull-in saddle node is less than that of the snap-through saddle nodes. For instance, for values of $h = 0.4$ and $\beta = 180$ this particular case appears. Two types of behaviours are possible in this case, as follows.

Case D.1: For small values of R or high values of μ, and provided that the dynamic response amplitude does not reach the critical values imposed by the snap-through homoclinic orbits, the system acts, in this case, as a regular resonator with a softening-type behaviour. The frequency response behaviour in this case is qualitatively similar to that of Case A.1 shown in Fig. 3.

Case D.2: When values of μ and R are appropriately selected to make the dynamic response amplitude to reach the snap-through critical value, the dynamic snap-through instability occurs. However, since the potential of the pull-in saddle is lower than that of the snap-though one, the system undergoes a direct pull-in. In other words, it is not possible in this case to have stable snap-through, and any dynamic instability will result in a dynamic pull-in. This is also the case when the response approaches the pull-in homoclinic orbit shown in Fig. 8, for values of $R = 0.02$, $\mu = 0.03$ and $\sigma = -0.16$.

4. Conclusions: A single degree of freedom reduced-order model is used to perform dynamic behaviour analysis of a shallow arch-shaped microbeam used as a MEMS resonator. Possible dynamic behaviours of the resonator are classified based on the shape of its potential function. Conditions for the appearance of various scenarios such as softening frequency response, dynamic snap-through, dynamic pull-in, large amplitude and chaotic vibrations are discussed.

It is shown that for small values of R (ratio of the AC voltage to DC voltage) the proposed arch acts as a typical resonator showing softening behaviour near its primary resonance. Once the response amplitude reaches the amplitude of the corresponding snap-through homoclinic orbit, the resonator undergoes either a chaotic behaviour (Case B), a dynamic snap-through (Case C) or a definite dynamic pull-in (Case D). In all cases, as the response amplitude reaches the pull-in homoclinic orbit, the dynamic pull-in instability occurs. Large amplitude of vibrations due to limit cycles in the phase planes are also possible for some types of potential function and excitation parameters (as discussed in cases B and C).

We have shown that in certain conditions the arch MEMS can possibly undergo chaotic vibrations. Moreover, we showed that the large amplitude vibrations of the resonator, which are practically important because of the enhanced gain of the resonator in such case, are possible to take place at Case B.3. Moreover, we have shown the hardening behaviour of the resonator in this case; the given discussion can be a justification for the already reported behaviour of the system [13, 14].

It is also shown that stable transitions between the fixed points are possible at certain conditions (Case C.2). According to the simulations of this particular case, vibrations of the resonator may jump from the vicinity of one stable point to the other due to resonance. This takes place only by the sweeping of the actuating AC frequency. This case was shown to be practical and interesting, especially for MEMS-based filters. We have shown that the system response in forward and backward frequency sweeps can differ. This phenomenon, which was recently observed experimentally [16], can be justified by the proposed simulations in Case C.2. Moreover, through the proposed simulations, we have shown that the hysteresis loops are the dominant behaviour of the bistable resonator. Therefore this nonlinear phenomenon can significantly affect the recently proposed filtering functionality of the bistable MEMS resonator, and should be considered in the design procedure of this family of MEMS-based filters.

Finally, we have shown that, in Category D, although the system is statically bistable, any snap-through motion will be immediately followed by the pull-in instability. Therefore, the bistable nature of the resonator in this case cannot be functionally beneficial.

5 References

[1] Ko J.S., Lee M.G., Han J.S., Go J.S., Shin B., Lee D.S.: 'A laterally-driven bistable electromagnetic microrelay', *ETRI J.*, 2006, **28**, pp. 389–392

[2] Park S., Hah D.: 'Pre-shaped buckled-beam actuators: theory and experiments', *Sens. Actuators A, Phys.*, 2008, **148**, (1), pp. 186–192

[3] Ko J.S., Lee M.L., Lee D.S., Choi C.A., Kim Y.T.: 'Development and application of a laterally driven electromagnetic microactuator', *Appl. Phys. Lett.*, 2002, **81**, (3), pp. 547–549

[4] Charlot B., Sun W., Yamashita K., Fujita H., Toshiyoshi H.: 'Bistable nanowire for micromechanical memory', *J. Micromech. Microeng.*, 2008, **18**, (4)

[5] Zhang Y., Wang Y., Li Z., Huang Y., Li D.: 'Snap-through and pull-in instabilities of an arch-shaped beam under an electrostatic loading', *J. Microelectromech. Syst.*, 2007, **16**, (3), pp. 684–693
[6] Medina L., Gilat R., Krylov S.: 'Symmetry breaking in an initially curved micro beam loaded by a distributed electrostatic force', *Int. J. Solids Struct.*, 2012, **49**, (13), pp. 1864–1876
[7] Krylov S., Seretensky S., Schreiber D.: 'Pull-in behavior and multistability of a curved microbeam actuated by a distributed electrostatic force'. IEEE 21st Int. Conf. Micro Electro Mechanical Systems, January 2008, pp. 499–502
[8] Krylov S., Ilic B.R., Schreiber D., Seretensky S., Craighead H.: 'The pull-in behavior of electrostatically actuated bistable microstructures', *J. Micromech. Microeng.*, 2008, **18**, (5)
[9] Krylov S., Dick N.: 'Dynamic stability of electrostatically actuated initially curved shallow micro beams', *Continuum Mech. Thermodyn.*, 2010, **22**, pp. 445–468
[10] Das K., Batra R.C.: 'Pull-in and snap-through instabilities in transient deformations of microelectromechanical systems', *J. Micromech. Microeng.*, 2009, **19**, p. 035008
[11] Mohammad T.F., Ouakad H.M.: 'Static, eigenvalue problem and bifurcation analysis of MEMS arches actuated by electrostatic fringing-fields', *Microsyst. Technol.*, 2014
[12] Casals-terré J., Fargas-marques A., Shkel A.M.: 'Snap-action bistable micromechanisms actuated by nonlinear resonance', *J. Microelectromech. Syst.*, 2008, **17**, (5), pp. 1082–1093
[13] Ouakad H.M., Younis M.I.: 'The dynamic behavior of MEMS arch resonators actuated electrically', *Int. J. Nonlinear Mech.*, 2010, **45**, pp. 704–713
[14] Younis M.I., Ouakad H.M., Alsaleem F.M., Miles R., Cui W.: 'Nonlinear dynamics of MEMS arches under harmonic electrostatic actuation', *J. Microelectromech. Syst.*, 2010, **19**, (3), pp. 647–656
[15] Ouakad H.M.: 'An electrostatically actuated MEMS arch band-pass filter', *Shock Vib.*, 2013, **20**, pp. 809–819
[16] Ouakad H.M., Younis M.I.: 'On using the dynamic snap-through motion of MEMS initially curved microbeams for filtering applications', *J. Sound Vib.*, 2014, **333**, (2), pp. 555–568
[17] Tajaddodianfar F., Nejat Pishkenari H., Hairi Yazdi M., Maani Miandoab E.: 'On the dynamics of bistable micro/nano resonators: analytical solution and nonlinear behavior', *Commun. Nonlinear Sci. Numer. Simul.*, 2015, **20**, (3), pp. 1078–1089
[18] Tajaddodianfar F., Hairi Yazdi M., Nejat Pishkenari H.: 'On the chaotic vibrations of electrostatically actuated arch micro/nano resonators: a parametric study', *Int. J. Bifurcation Chaos*, 2015

doi: 10.1049/mnl.2015.0087